Available online at www.sciencedirect.com

ScienceDirect

Procedia Engineering 2 (2010) 2199–2208

Procedia Engineering

www.elsevier.com/locate/procedia

Fatigue 2010

Cyclic behavior and microstructural stability of ultrafine-grained AA6060 under strain-controlled fatigue

K. Hockauf[a]*, T. Niendorf[b], S. Wagner[a], T. Halle[a], L.W. Meyer[c]

[a]*Institute of Materials Science and Engineering, Chemnitz University of Technology, Erfenschlager Str. 73; D-09125 Chemnitz, Germany*
[b]*Lehrstuhl für Werkstoffkunde (Materials Science), University of Paderborn, Pohlweg 47-49, D-33095 Paderborn, Germany*
[c]*Nordmetall Research and Consulting GmbH; Hauptstraße 16; D-09221 Adorf (Neukirchen), Germany*

Received 26 February; revised 11 March; accepted 15 March

Abstract

The strain-controlled fatigue behavior of AA6060, a precipitation hardening aluminum alloy, was investigated in ultrafine-grained (UFG) conditions after severe plastic deformation (SPD) by equal-channel angular pressing (ECAP). Two as-processed conditions, representing different stages of strain hardening and grain refinement as well as a ductility-optimized condition, achieved by a combined ECAP and aging treatment were considered. Low-voltage scanning transmission electron microscopy on samples stopped at characteristic stages of the fatigue process was applied to investigate the microstructural development. The as-processed as well as the optimized condition showed cyclic softening, which was found to be dependent on the amount of pre-strain induced by ECAP processing. This is linked to dynamic recovery processes in the microstructure, indicated by a clearer distinction of grain boundaries and a reduction of dislocations in the grain interior. For all applied plastic strain amplitudes, ranging from $\Delta\varepsilon_{pl}/2 = 1x10^{-3}$ to $5x10^{-3}$, the fatigue life of the ductility-optimized condition did not reach that of the severely work-hardened counterpart. For explaining this unexpected result, the differing (size-dependent) effectiveness of precipitates for the pinning of dislocations during cyclic loading was considered.

Keywords: cyclic stress-strain response; fatigue life; equal-channel angular pressing (ECAP); precipitation hardening aluminum alloy; ultrafine-grained; ductility; cyclic softening; dynamic recovery

1. Introduction

During the last decade, starting 20 years after the pioneer work of Segal in the early 1980s [1], the properties of ultrafine-grained (UFG) materials processed by methods of severe plastic deformation (SPD) have gained an enormously growing interest. Among numerous different SPD technologies, equal-channel angular pressing (ECAP), where a bulk billet is repetitively pressed through an L-shaped channel and subjected to a large simple shear deformation, of typically ~ 1.1 per pass, has become one of the most widely applied methods. For all SPD methods, the procedure of grain refinement is understood as a self-organized arrangement of dislocations in (sub-)grain boundaries which is enforced by the high dislocation density introduced during the cold working process.

* Corresponding author. Tel.: +49-371-531-36812; fax: +49-371-531-836812.
E-mail address: kristin.hockauf@mb.tu-chemnitz.de

1877-7058
doi:10.1016/j.proeng.2010.03.236

Starting with low-angle grain boundaries (LAGB), during further deformation, newly generated and integrated dislocations increase the misorientation angles between the sub-grains and lead to their transformation into high-angle grain boundaries (HAGB). With this procedure, an ultrafine-grained microstructure is generated and the strength of the material is increased – higher than it would be possible by means of conventional thermo-mechanical treatments. Furthermore, the density of dislocations in the grain interior contributes to the strengthening effect.

Thus, ECAP processing exerts an impressively positive influence on stress-controlled fatigue properties and enhanced fatigue strengths have been reported numerously for different metallic materials [2-4]. By contrast, the ductility and – inevitably combined – the strain-controlled fatigue life is decreased drastically. In the case of wavy-slip materials, like aluminum, a reduced cyclic stability combined with cyclically induced grain growth for high-purity materials, and early strain localization caused earlier failure of the UFG microstructures compared to their conventionally grained (CG) counterparts [5, 6].

In order to overcome this drawback and regain a certain amount of ductility, an annealing treatment after ECAP was proposed and found to be effective for pure as well as alloyed Al and Cu [4, 7-10]. However, as it is based on recovery processes, the success of this method is inevitably combined with a loss in strength. For precipitation hardening aluminum alloys, Kim et al. [11] found a promising method for preserving an increased strength as well as a moderate ductility. They performed low-temperature ECAP processing in a solid-solution heat treated condition and conducted a short low-temperature aging treatment subsequently. With this method, they enabled strengthening processes such as the formation of very fine particles as well as softening recovery processes such as a decrease in the dislocation density to occur at the same time.

For obtaining the optimized condition presented in this paper, this strategy was employed. The processing strategy was chosen based on preliminary studies on the monotonic stress-strain behavior and high cycle fatigue performance [12, 13]. Furthermore, two as-processed conditions with different states of grain refinement, after two and eight repetitive pressings, were investigated. The former represents the as-processed reference for the optimized condition, the latter a condition of completely homogeneous grain refinement. For comparison with the initial material behavior, the conventionally grained material in the technically relevant peak-aged condition (T6) was employed.

2. Experimental procedure

2.1. ECAP processing and conditions

The investigated material is a precipitation hardening Al-Mg-Si aluminum alloy of commercial purity, designated as AA6060. ECAP processing was performed in a die-set with an intersection angle of 90 °, resulting in an equivalent strain of ~1.1 per pass. The pressings were done at room temperature, applying a backpressure of 70 MPa after the 6^{th} pass, to ensure homogeneous deformation and to prevent cracking. For an effective microstructural refinement, pressings were done following route E [14]. Starting with the material in the peak-aged (T6) temper, two and eight pressings were performed, resulting in an equivalent plastic strain of $\varphi = 2.3$ and $\varphi = 9.2$, respectively. These conditions are hereafter referred to as “E2” and “E8”.

For obtaining the optimized condition, the material was solid-solution heat treated at 525 °C for 60 minutes and water-quenched to room temperature. After that, the billets were ECAP-processed for two passes following Route E, applying a backpressure of 70 MPa to ensure fully homogeneous deformation. Subsequently, a short aging was conducted at 170 °C for 18 minutes. Those parameters were chosen referring to an investigation on the post-ECAP precipitation kinetics of this material, where this particular aging treatment led to a post-ECAP peak age condition with an excellent combination of strength and ductility [12]. The optimized condition will hereafter be referred to as “E2 opt”.

2.2. Materials testing

Monotonic tensile tests were conducted at an initial strain rate of 10^{-3} s^{-1}, using round samples with a diameter of 3.5 mm and a gauge length of 10.5 mm. For (total) strain-controlled fatigue tests, round samples with a gauge diameter of 3.5 mm and a length of 6 mm were used. A miniature extensometer with a gauge length of 3 mm was

directly attached to the specimens for the sake of accurate strain measurement. The experiments were carried out in symmetric push-pull (R = -1) at a constant strain rate of $2.4x10^{-2}$ s^{-1} in a MTS 810 servo-hydraulic test system with constant plastic strain amplitudes $\Delta\varepsilon_{pl}/2$ ranging from $1x10^{-3}$ to $5x10^{-3}$. The monotonic as well as the fatigue tests were performed at RT.

For the plastic strain amplitude of $5x10^{-3}$, the cyclic softening behavior was evaluated from the region of linear decline, ranging from cycles 50 to 300. The cyclic softening rates, displayed as $d(\Delta\sigma/2)/dN$ in Fig. 2, were calculated from a linear curve fit in this region.

2.3. Microstructural investigations

For documenting the microstructural development, samples fatigued at $\Delta\varepsilon_{pl}/2 = 5x10^{-3}$ were stopped during the onset of microstructural activities at N=5 and in the region of linear softening (saturation for T6) at N=150 cycles. Specimens for scanning transmission electron microscopy (STEM) investigations were taken. Together with specimens prior to fatigue and after fracture, they were first twin jet electropolished and subsequently polished using an Ar-ion beam. Investigations were conducted in a scanning electron microscope NEON40EsB from ZEISS, operating at an acceleration voltage of 30 kV.

3. Microstructures prior to fatigue

STEM micrographs of microstructures prior to fatigue are shown in Fig. 1. Below, microstructural characteristics relevant for the fatigue behavior will be discussed; letters in brackets refer to sections in this figure.

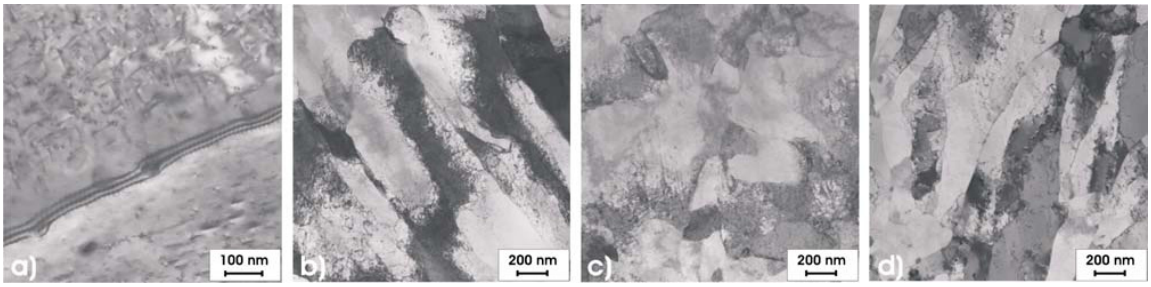

Fig. 1. Microstructure prior to fatigue (STEM) (a) initial T6; (b) E2; (c) E8; (d) E2 opt.

3.1. T6 initial condition (a):

The initial microstructure consists of globular grains in the size of 110 μm. The material was investigated in the peak age condition, where characteristically the precipitates are undergoing a transition from coherent β"-needles to semi-coherent β'-rods. In the present microstructure both types are expected to exist, though the cyclic stress-strain behavior indicates the presence of a majority of the non-shearable β'-rods. Aside, larger precipitates containing iron (impurity) and silicon have formed, mainly at grain boundaries, binding the silicon in their vicinity and leading to the formation of precipitate-free zones.

3.2. E2 and E8 (b+c):

In the micrographs of these conditions precipitates can only be observed when they interact with dislocations. Otherwise, their contrasts, induced by microstructural distortion, are outshined by the much more intense local stress contrasts of the ECAP-induced dislocation structures. In these micrographs, the formation of (sub-)grains can be seen, as well as a high density of remnant dislocations in the grain interior.

In condition E2 (Fig. 1b), the grains are elongated, stretched out in the direction of shear. In the first and second pass of ECAP following route E, the material is deformed forth (1st) and back (2nd) along the same shearplane.

As every two passes the billet is rotated for 90 ° around the extrusion axis, the microstructure of E8 is completely pervaded by shearplanes, which results in a globular structure. Electron backscatter diffusion (EBSD) analysis showed that after two passes, only 10 % of the grain boundaries revealed a high-angle misorientation, whereas after 8 passes, as much as 30 % were HAGBs [15].

According to the work of Valiev et al. [16] and Chuvil'deev et al. [17], the grain boundaries formed by severe plastic deformation exhibit a non-equilibrium constitution. It accrues from the so called *surplus free volume*, which is introduced by each lattice defect (dislocation and/ or vacancy) which is moving into a grain boundary and added to the boundary's geometrically necessary volume. The density of defects accumulated in a grain boundary, and the surplus free volume arising from it, depends on the amount of strain introduced by ECAP, the processing temperature and strain rate. Thus, for equal strain rates and processing temperatures, the defect-induced surplus free volume increases with an increasing number of ECAP passes. Therefore, during repetitive ECAP processing, the grain boundaries transform to a more and more non-equilibrium state.

3.3. E2 opt (d)

As it was solution-treated prior to ECAP, and peak-aged after the deformation, the optimized condition consists of a somewhat different microstructural configuration that is formed during the aging treatment. While its structure after ECAP and prior to aging contained a high fraction of non-equilibrium grain boundaries and a high inherent dislocation density, the thermal activation during aging facilitated first recovery processes. Dislocations were annihilating and forming LAGBs in a process known as polygonization. These softening processes were superposed by the strengthening effect of the β"-precipitates, which started to form with an extraordinary velocity due to the increased number of diffusion pathways. A very fine size and distribution of those precipitates is achieved since they are arising from numerous nucleation sites in the highly distorted microstructure. The aging process was stopped when both competing processes where balancing each other, e.g. before the softening effect could prevail. As a result, this condition shows a recovered but not yet recrystallized microstructure with a high number of LAGBs and finely distributed precipitates. Compared to the as-processed conditions, the defect annihilation during aging decreases the dislocation density in the grain interior as well as the amount of surplus free volume in the grain boundaries. In this recovered microstructure grain boundaries appear in a less blurred, more pronounced characteristic.

4. Monotonic stress-strain response

Results from tensile tests of the investigated conditions are shown in Fig. 2 and Tab. 1. For comparing ductility characteristics, the uniform elongation (UE) was chosen as a measure rather than the elongation to failure.

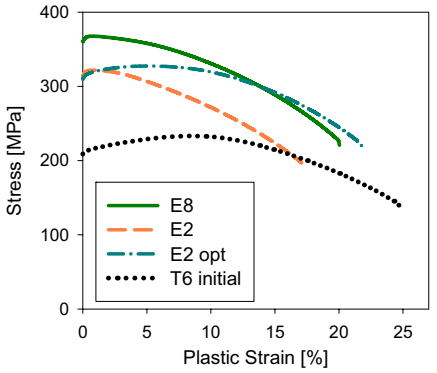

Fig. 2. Tensile stress-strain behavior.

It quantifies the strain before necking of the sample and represents the formability before the onset of strain localization. Further, the yield ratio as a measure of strain hardening capability was considered.

When compared with the initial material, the as-processed conditions E2 and E8 reach a yield strength (YS) which is 50 % and 70 % higher, respectively. This is a remarkable result, since the T6 condition represents the maximum strength that can be reached by a conventional heat treatment.

As a consequence of extreme cold working, ECAP processing also led to a significant decrease in ductility to approximately 1.0 % uniform elongation for both as-processed conditions. Also their yield ratios of 0.97 and 0.98 show that the strain hardening capability has been almost exhausted during ECAP.

The optimized condition reaches a YS and UTS that is in the range of the as-processed E2, whereas its ductility is recovered to 5.4 % UE. This indicates a positive result for the chosen optimization strategy. Nevertheless, considering the yield ratio of 0.94, the strain hardening capability is still strongly limited.

Table 1. Tensile stress-strain behavior.

Condition	YS (*MPa*)	UTS (*MPa*)	UE (*%*)	Elongation to failure (*%*)	Yield ratio (*YS/UTS*)
T6 initial	208	233	9.1	25.6	0.89
E2	316	322	1.0	17.4	0.98
E2 opt	310	328	5.4	22.0	0.94
E8	358	368	1.0	20.3	0.97

5. Strain-controlled fatigue

The fatigue behavior at a constant plastic strain amplitude of $\Delta\varepsilon_{pl}/2 = 5x10^{-3}$ is displayed in Fig. 3. The T6 initial condition exhibits a short region of cyclic hardening, leading to saturation, as it is typical for materials containing non-shearable precipitates [18, 19]. For both as-processed conditions E2 and E8, the highly distorted microstructure far from equilibrium exerts a high driving force for dynamic isothermal recovery. Both conditions show a distinctive softening behavior which is known as a characteristic feature of ECAP-processed wavy-slip materials [20].

Activated by the energy imposed during plastic straining, recovery processes take place, such as the movement of dislocations into grain boundaries, defect annihilation in the grain interior, and the reduction of the non-equilibrium state of grain boundaries. At the very beginning of cycling, within the first ten reversals, those softening processes proceed rapidly and are then decelerated to a linear decline. It is assumed that the change of the strain path from simple shear (ECAP) to tension-compression (fatigue) causes this behavior. Whilst the majority of the slip systems had been activated and extensively used for the shear deformation during ECAP, the change of strain path in the very first cycle of tension-compression fatigue activates dislocation movement on other, differently oriented slip systems. Dislocations are able to move comparatively free on them and, as a result, recovery processes proceed rather fast. Comparing E2 and E8, this initial recovery is more pronounced for the condition with higher ECAP pre-strain. After the initial few reversals, when the newly activated slip systems are also extensively strained and the primarily evolved annihilation lower the driving force for further recovery, the section of linear softening sets in.

Contrary to that, the optimized condition does not show such an accelerated softening at the onset of cyclic straining, as recovery processes were already activated during aging. In contrast, a short section of cyclic hardening can be observed, caused by dislocation multiplication and storage. Nevertheless, the strain hardening capability seems to be already exhausted after the first ten cycles. In the following stage of linear softening the curves of E2 and E2 opt proceed congruently. This means that the thermally activated recovery in E2 opt only influences the very first stage of cyclic behavior and does not prevent further softening.

In the following stage, approximately beginning in cycle ten, all of the ECAP-processed conditions (as-processed as well as optimized) exhibit a softening behavior which can be described by a linear trend. Within this region, the softening rates displayed in Fig. 3 evidently increase with the amount of ECAP pre-strain (compare E2 and E8). However, as for E2 and E2 opt differences in the state of recovery are already leveled out within the first few cycles, their softening rates tend to be equal in this stage. Compared to the T6 initial condition, the differences in the softening behavior of the ECAP-processed conditions are only of a minor significance. The as-processed conditions as well as the optimized condition are prone to cyclic softening, whereby neither the grain boundary characteristics

(LAGB/ HAGB) nor the induced recovery prior to cycling (in E2 opt) exert a major influence. This is somehow unexpected, since it was shown that post-ECAP annealing treatments can be effective to limit cyclic softening [9, 10]. Additionally, several studies have shown the beneficial influence of a higher amount of HAGB [21, 22], which could not be confirmed by comparison of the E2 and the E8 condition in this study. However, the abovementioned studies on the influence of grain boundary misorientations were conducted on an IF steel and pure Cu, excluding the substantial influence of precipitates.

These results indicate that, during cyclic loading, the role of precipitates in the microstructure exerts an influence that outranges the effects of grain boundary misorientation and the ductility enhancing optimization treatment.

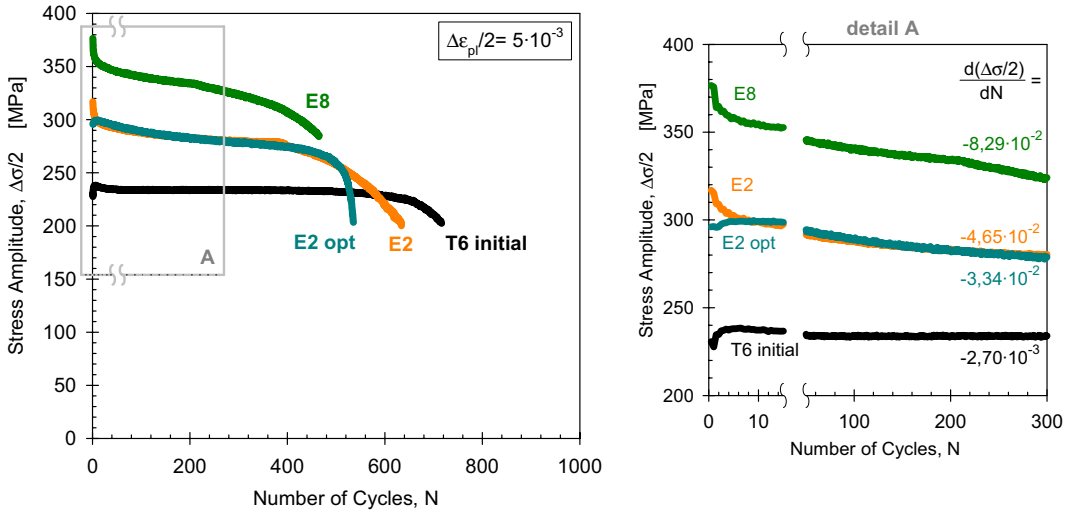

Fig. 3. Cyclic stress-strain response at $\Delta\varepsilon_{pl}/2 = 5x10^{-3}$.

6. Microstructural evolution during fatigue

In this section, the cyclic stress-strain response interpreted above will be complemented with microstructural investigations on fatigued samples, stopped at characteristic stages during the fatigue process and after fracture. Fig. 4 shows the microstructural evolution at $\Delta\varepsilon_{pl}/2 = 5x10^{-3}$ of all conditions under investigation by representative micrographs. Processes happening in one particular condition are displayed from left to right, starting with the initial microstructure, the completion of the first stage after N=5, the stage of linear softening (stable behavior for initial T6) and ending with the microstructure of a fractured sample at $N=N_f$.

In the T6 initial condition prior to fatigue, the stress fields of ordered β" and β'-precipitates are visible. A small number of dislocations, nucleated during precipitation, can be observed in between the β'-rods. With the beginning of cycling, the dislocation density increases, and dislocations are pinned by precipitates, forming curved configurations. A net of tangled dislocations evolves throughout the grains, at N=5 still in development, at N=150 already in the final shape. If dislocations are not pinned, they leave Orowan loops after a bypass process. Those configurations are typically observed for alloys with non-shearable precipitates [18, 23]. The effect of a precipitate-free zone can be seen in the micrographs at N=5 and N=150. Large Fe- and Si-rich precipitates have formed at the grain boundary, binding silicon and thus inhibiting the formation of strengthening precipitates (β" or β') in their vicinity. Thus, no dislocations are pinned and the dislocation structures terminate at the precipitate-free zone. Once formed, the net-like structure remains stable until fracture.

While strain hardening is based on an increasing dislocation density in the grain interior, softening processes can be observed when indications for dynamic recovery are present. They can be observed when formerly blurred grain boundaries appear more defined and the dislocation density in the grain interior decreases.

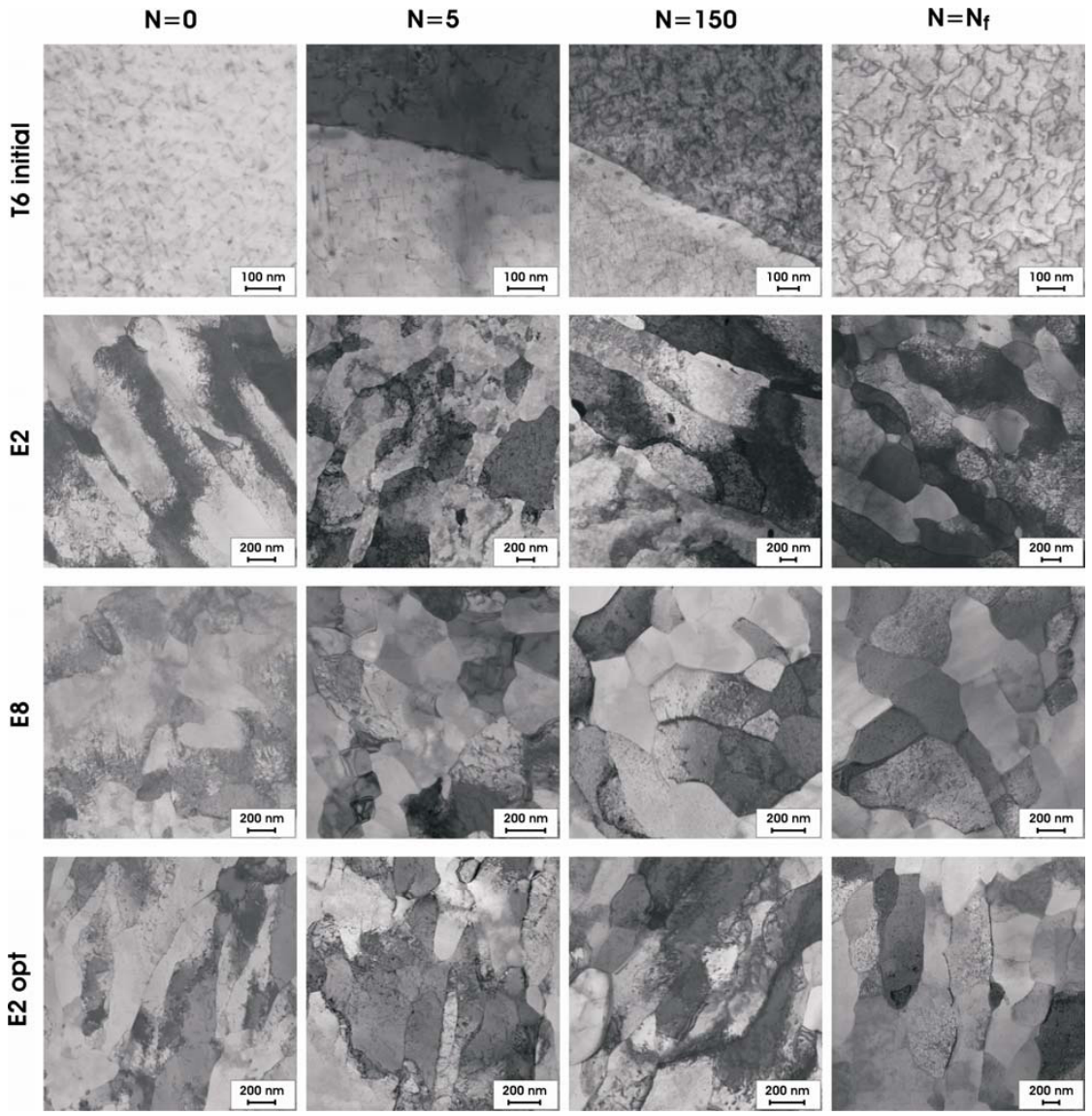

Fig. 4. Microstructural evolution at $\Delta\varepsilon_{pl}/2 = 5x10^{-3}$, STEM micrographs.

Dynamic recovery processes are activated by the energy imposed during cyclic straining, when mobilized dislocations are enabled to move and annihilate. Thus, recovery in the grain interior as well as the non-equilibrium grain boundaries takes place.

In this context, it should be mentioned, that grain growth due to strain induced recovery, as it is observed for pure ECAP materials, is not the case for the utilized alloy. The presence of precipitates and impurities stabilizes moving grain boundaries and prevents grain growth.

For the as-processed conditions, the microstructural changes due to dynamic recovery are most pronounced in the first few cycles (N=0 to N=5). Beyond that, no significant changes can be observed. Keeping this in mind, it can be

explained why for the optimized condition almost no microstructural changes are visible during fatigue. The energy imposed during aging already caused the formation of a recovered initial microstructure, characterized by clearly pronounced grain boundaries and a lower density of remnant dislocations in the grain interior. Within the first cycles, the observed hardening should result in an increase in the dislocation density for N=5, however, only to the extent of the T6 initial condition or even lower. Those small changes cannot be clearly stated from the micrographs. For the optimized condition also after N=5, the microstructural features cannot be clearly related to either the aging recovery prior to, or the dynamic recovery during fatigue.

It is remarkable that only the CG condition shows the development of significant dislocation structures during cycling. For the as-processed conditions, tangles of dislocations which were initiated during ECAP can be observed in the (sub-)grain interiors prior to cycling. During the fatigue process they are loosened step by step and dissolved. This effect can be seen clearly for E8 and slightly less pronounced for E2. The same observations apply to the E2 opt condition, with the exception that the dislocation density is already lowered at the beginning of cycling.

This indicates that the precipitates in the as-processed as well as the optimized condition are not effective to pin dislocations and constrain their annihilation or dissolution in grain boundaries. Provided that the precipitates which were present in the initial microstructure are fragmented by ECAP, as it is reported in [24-26], their decreased size, making them penetrable for dislocations, can be assigned as a possible reason for the observed behavior in the as-processed conditions E2 and E8. Also for the optimized condition E2 opt, the assumption of penetrable (=coherent) precipitates is reasonable, as the peak strength is related to coherent precipitates. Additionally, precipitate characteristics after ECAP processing are known to be extraordinarily fine [25, 27].

Concluding this argumentation, the investigated conditions can be brought in the following order according to the size of their precipitates, starting with the largest: T6 → E2 → E8 / E2 opt. This matches in reverse order the ranking in which they exhibit cyclic softening.

7. Coffin-Manson plot

For comparison of the fatigue life, the cycles to failure of the individual curves from Fig. 3 are displayed in a Coffin-Manson plot in Fig. 5, complemented by fatigue lives at two lower plastic strain amplitudes. The results are to some extent contradictory to the expectations based on the literature. For a first point, differences in fatigue life of the CG and the UFG conditions appear not as significant as expected based on [4] and [8]. For a second point, derived from the regained ductility in monotonic tensile tests, an enhancement of the fatigue life would be expected for the optimized condition E2 opt, which is not the case in Fig. 5.

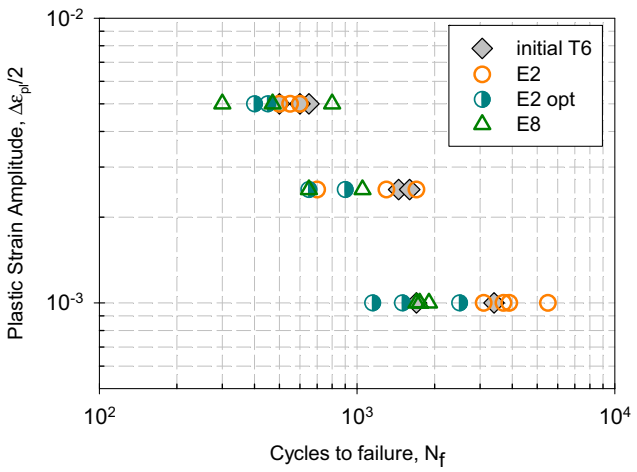

Fig. 5. Coffin-Manson plot, all experimental data is displayed.

The first issue can be solved when it is taken into account that already the initial condition reveals the characteristics of a material which is aged to peak strength and thus exhibits only a limited ductility and strain hardening capability. In many comparative studies, the CG conditions are either soft-annealed, containing coarse, incoherent particles, or very soft and ductile by nature as they are pure materials. Having this as a measure in mind, it can be estimated that the improvement in uniform elongation and yield ratio of the optimized condition E2 opt was not significant enough to cause a considerable improvement in strain-controlled fatigue life. Furthermore, an analysis of the precipitate characteristics seems to be necessary when dealing with the question why E2 opt does not show the expected improvement. As discussed above, the precipitates are expected to be fragmented by ECAP processing and thus easier penetrable for dislocations, with increasing ease for a high number of passes. The presence of such shearable particles will lead to the formation of deformation bands under cyclic loading [28], which represent localized slip and are starters for local deterioration and damage. Taking into account the assumed size of the precipitates, especially E2 opt and E8 should be prone to this damage mechanism, which is also shown by their early failure in the Coffin-Manson plot.

8. Summary

The cyclic stress-strain response of an Al-Mg-Si precipitation hardening aluminum alloy in the initial peak-aged condition, in two as-processed ECAP conditions as well as a ductility-optimized condition was investigated. Major points of research were the influence of ECAP pre-strain, e.g. numbers of passes, and the effect of an aging treatment prior to fatigue. The investigations on the cyclic stress-strain response were complemented with microstructural investigations on samples stopped at characteristic stages in the fatigue process and after fracture.

The results can be concluded as follows:

- Continuous cyclic softening appears for the as-processed ECAP materials. It can be divided into two stages: an accelerated softening during the very first few cycles (caused by the change in strain path and the corresponding activation of new slip systems) and a following linear decline. In both stages, softening is most pronounced for the E8 condition with the highest amount of ECAP pre-strain.

- For the optimized condition, in the first stage, a slight hardening can be observed, followed by a linear softening with a cyclic stress-strain response which is congruent to the as-processed counterpart E2. Thus, the thermally induced recovery does not prevent cyclic softening in the ongoing fatigue process.

- Although the optimized condition E2 opt shows a higher ductility and strain hardening capability in monotonic loading than its as-processed counterpart E2, its performance in strain-controlled fatigue life remains below the expectations. This is supposedly caused by the formation of extraordinarily fine precipitates after ECAP, which make the E2 opt condition more prone to shear localization in deformation bands.

Acknowledgements

The authors thank Mrs. A. Schulze for the accurate specimen preparation for STEM measurements. This work was supported by the „Deutsche Forschungsgemeinschaft“ within the framework of „Sonderforschungsbereich 692: Hochfeste aluminiumbasierte Leichtbauwerkstoffe für Sicherheitsbauteile“.

References

[1] Segal VM, Reznikov AE, Drobyshevskiy AE, Kopylov VI. Plastic Working of Metals by Simple Shear. *Russ Metall (english translation)* 1981;**1**:99-105.

[2] Vinogradov A. Fatigue limit and crack growth in ultra-fine grain metals produced by severe plastic deformation. *J Mater Sci* 2007;**42**:1797-808.

[3] Xu CZ, Wang QJ, Zheng MS, Zhu JW, Li JD, Huang MQ et al. Microstructure and properties of ultra-fine grain Cu-Cr alloy prepared by equal-channel angular pressing. *Mater Sci Eng A* 2007;**459**:303-8.

[4] Höppel HW. Mechanical properties of ultrafine-grained metals under cyclic and monotonic loads: An Overview. *Mater Sci Forum* 2006;**503-504**:259-66.

[5] Kunz L, Lukáš P, Svoboda M. Fatigue strength, microstructural stability and strain localization in ultrafine-grained copper. *Mater Sci Eng A* 2006;**424**:97-104.

[6] Höppel HW, Brunnbauer M, Mughrabi H, Valiev RZ, Zhilyaev AP. Cyclic deformation behavior of ultrafine grain size copper produced by equal channel angular extrusion. *Materialsweek 2000* (www.materialsweek.org/proceedings, 2000).

[7] Mughrabi H, Höppel HW, Kautz M. Fatigue and microstructure of ultrafine-grained metals produced by severe plastic deformation. *Scr Mater* 2004;**51**:807-12.

[8] Maier HJ, Gabor P, Gupta N, Karaman I, Haouaoui M. Cyclic stress-strain response of ultrafine grained copper. *Int J Fatigue* 2006;**28**:243-50.

[9] Höppel HW, Kautz M, Xu C, Murashkin A, Langdon TG, Valiev RZ et al. An overview: Fatigue behaviour of ultrafine-grained metals and alloys. *Int J Fatigue* 2006; **28(9)**:1001-10.

[10] Patlan V, Vinogradov A, Higashi K, Kitagawa K. Overview of fatigue properties of fine grain 5056 Al-Mg alloy processed by equal-channel angular pressing. *Mater Sci Eng A* 2001;**300**:171-182.

[11] Kim JK, Kim HK, Park JW, Kim WJ Large enhancement in mechanical properties of the 6061 Al alloys after a single pressing by ECAP. *Scr Mater* 2005; **53(10)**:1207-11.

[12] Hockauf M, Meyer LW, Zillmann B, Hietschold M, Schulze S, Krüger L. Simultaneous improvement of strength and ductility of Al-Mg-Si alloys by combining equal-channel angular extrusion with subsequent high-temperature short-time aging. *Mater Sci Eng A* 2009;**503**:167-71.

[13] Hockauf K, Meyer LW, Halle T, Hockauf M. Crack growth and high cycle fatigue behaviour of an AA6060 aluminium alloy after ECAP combined with a subsequent heat treatment, *Materialwiss Werkstofftech* 2009;**40**:493-9.

[14] Barber RE, Dudo T, Yasskin PB, Hartwig KT. Product yield for ECAE processing. *Scr Mater* 2004;**51**:373-7.

[15] Hockauf M, Meyer LW, Halle T, Kuprin C, Hietschold M, Schulze S et al. Mechanical properties and microstructural changes of ultrafine-grained AA6063T6 during high-cycle fatigue. *Int J Mater Res* 2006;**97**:1392-1400.

[16] Valiev RZ, Gertsman VY, Kaibyshev OA, Khannanov S.K. Non-Equilibrium State and Recovery of Grain Boundary Structure. *Phys Status Solidi* A 1983;**77**:97-105.

[17] Chuvil'deev VN, Kopylov VI, Zeiger W. A theory of non-equilibrium grain boundaries and its applications to nano- and micro-crystalline materials processed by ECAP. *Ann Chim Sci Mat* 2002;**27**:55-64.

[18] Calabrese C, Laird C. Cyclic stress-strain response of two-phase alloys Part II. Particles not penetrated by dislocations. *Mater Sci Eng* 1974;**13**:159-74

[19] Jain M. Micromechanical stresses during low cycle fatigue of an overaged Al-Mg-Si alloy. *Fatigue Fract Eng Mater Struct* 1992;**15**:33-42.

[20] Vinogradov A, Hashimoto S. Multiscale phenomena in fatigue of ultra-fine grain materials - An overview. *Mater Trans* 2001;**42**:74-84.

[21] Niendorf T, Canadinc D, Maier HJ, Karaman I. On the Microstructural Stability of Ultrafine-Grained Interstitial-Free Steel under Cyclic Loading. *Metall Mater Trans A* 2007;**38**:1946-55.

[22] Canadinc D, Maier HJ, Haouaoui M, Karaman I. On the cyclic stability of nanocrystalline copper obtained by powder consolidation at room temperature. *Scr Mater* 2008;**58**:307-10.

[23] Jain M. TEM study of microstructure development during low-cycle fatigue of an overaged Al-Mg-Si alloy. *J Mater Sci* 1992;**27**:399-407.

[24] Xu C, Furukawa M, Horita Z, Langdon TG. Using ECAP to achieve grain refinement, precipitate fragmentation and high strain rate superplasticity in a spray-cast aluminum alloy. *Acta Mater* 2003;**51**:6139-49.

[25] Roven HJ, Liu M, Werenskiold JC. Dynamic precipitation during severe plastic deformation of an Al-Mg-Si aluminium alloy. *Mater Sci Eng A* 2008;**483-484:** 54-8.

[26] Kang SB, Lim CY, Kim HW, Mao J. Microstructure Evolution and Hardening Behavior of 2024 Aluminum Alloy Processed by the Severe Plastic Deformation. *Mater Sci Forum* 2002;**396-402**:1163-8.

[27] Cai M, Field DP, Lorimer GW. A systematic comparison of static and dynamic ageing of two Al-Mg-Si alloys. *Mater Sci Eng A* 2004;**373**:65-71.

[28] Calabrese C, Laird C. Cyclic stress-strain response of two-phase alloys Part I. Microstructures containing particles penetrable by dislocations. *Mater Sci Eng* 1974;**13**:141-57.